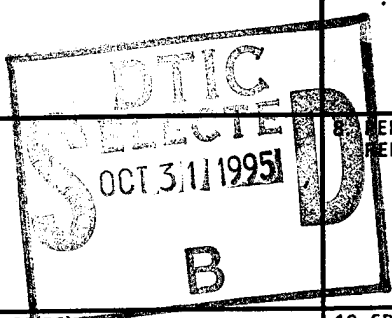


REPORT DOCUMENTATION PAGE			Form Approved OMB No. 0704-0188
<small>Public reporting burden for this collection of information is estimated to average 1 hour per response, including the time for reviewing instructions, searching existing data sources, gathering and maintaining the data needed, and completing and reviewing the collection of information. Send comments regarding this burden estimate or any other aspect of this collection of information, including suggestions for reducing this burden, to Washington Headquarters Services, Directorate for Information Operations and Reports, 1215 Jefferson Davis Highway, Suite 1204, Arlington, VA 22202-4302, and to the Office of Management and Budget, Paperwork Reduction Project (0704-0188), Washington, DC 20503.</small>			
1. AGENCY USE ONLY (Leave blank)	2. REPORT DATE 9/13/95	3. REPORT TYPE AND DATES COVERED Reprint	
4. TITLE AND SUBTITLE Optical-to-microwave Frequency Chain Utilizing a Two-laser-based Optical Parametric Oscillator Network		5. FUNDING NUMBERS DAAH04-93-G-0399	
6. AUTHOR(S) N.C. Wong			
7. PERFORMING ORGANIZATION NAME(S) AND ADDRESS(ES) Research Laboratory of Electronics Massachusetts Institute of Technology 77 Massachusetts Avenue Cambridge, MA 02139-4307			
8. PERFORMING ORGANIZATION REPORT NUMBER		9. SPONSORING/MONITORING AGENCY NAME(S) AND ADDRESS(ES) U. S. Army Research Office P. O. Box 12211 Research Triangle Park, NC 27709-2211	
10. SPONSORING/MONITORING AGENCY REPORT NUMBER ARO 31413.6-PH		11. SUPPLEMENTARY NOTES The view, opinions and/or findings contained in this report are those of the author(s) and should not be construed as an official Department of the Army position, policy, or decision, unless so designated by other documentation.	
12a. DISTRIBUTION/AVAILABILITY STATEMENT Approved for public release; distribution unlimited.		12b. DISTRIBUTION CODE	
13. ABSTRACT (Maximum 200 words) <p>Abstract. A method for building an optical-to-microwave frequency chain and for measuring optical frequencies relative to the cesium primary frequency standard is described. Based on optical frequency division via parametric oscillators, the concept is to generate two known ratios ($1/2$ and $4/9$) of an optical calibration frequency f_1 whose frequency difference is measured relative to the cesium clock. The ($1/2$) ratio is obtained by either a 2:1 frequency division of f_1 or second-harmonic generation of ($1/2$) f_1. The ($4/9$) ratio of f_1 can be generated with a 3:1 frequency divider driven by a second laser at f_2 that is chosen to be near ($2/3$) f_1, which in turn is obtained with a f_1-pumped 3:1 frequency divider. A set of auxiliary Optical Parametric Oscillators (OPOs) with outputs centered at ($1/2$) f_1 is used to facilitate the difference-frequency measurement between the two ratios. A practical configuration utilizing a YAG and a Ti: Al₂O₃ laser and its application to a number of precision measurements of interest are presented.</p>			
14. SUBJECT TERMS DTIC QUALITY INSPECTED 5		15. NUMBER OF PAGES	
17. SECURITY CLASSIFICATION OF REPORT UNCLASSIFIED		16. PRICE CODE	
18. SECURITY CLASSIFICATION OF THIS PAGE UNCLASSIFIED		19. SECURITY CLASSIFICATION OF ABSTRACT UNCLASSIFIED	
20. LIMITATION OF ABSTRACT UL			

19951030 043

Optical Parametric Oscillators (OPOs) [4], and sum- and difference-frequency mixing [5,6]. The proposed frequency-counting systems are envisioned to be all-solid-state and compact, and they are potentially useful not only in frequency metrology and precision measurements but also in the area of optical communication networks.

One of the proposed methods employs a parallel network of OPOs driven by a single calibration laser with the ratios $a = 2/3$ and $b = 1/2$ [4]. Unlike the conventional frequency chain and other proposed methods, this one-laser OPO network does not require additional transfer laser oscillators. Instead, OPOs are used for generating the ratios and for measuring the difference frequency $(a - b)f$. OPO frequency division with a pump-frequency to output-frequency ratio of 2:1 has been reported [7]. In a 2:1 divider, the beat between the two nearly equal output frequencies is phase locked to a microwave source. A 3:1 OPO divider has not been demonstrated but it can be implemented in the following way. In a 3:1 divider, the output frequencies are related by a factor of two. Therefore, the higher-frequency output and the second harmonic of the lower-frequency output can be phase locked to yield the exact ratio of 3:1 between the pump and the lower-frequency output. This phase locking can be accomplished either external or internal to the OPO. Because parametric interactions are non-resonant, OPOs can be very low noise devices. Together with their high conversion efficiency and wide tunability, OPOs are potentially more suitable than lasers for use in frequency chains.

A major disadvantage of this one-laser-based OPO method is that, in addition to the two OPOs that are used to generate the markers $(1/2)f$ and $(2/3)f$, 10 or more OPOs may be needed for measuring the frequency difference between the two markers. It is therefore interesting to investigate the feasibility of using two ratios that are closer than $(1/2)$ and $(2/3)$ in order to reduce the number of required OPOs. Also, while it is obvious that at least one laser is needed for the calibration, it is instructive to examine if there is any advantage in employing an additional laser as a transfer oscillator.

In this paper, we propose a two-laser-based OPO frequency synthesis chain. By using a second laser, we will show that the ratios $(1/2)$ and $(4/9)$ can be generated with a difference-frequency ratio of $(1/18)$, which is 6 times smaller than the corresponding ratio of $(1/3)$ for the case of the one-laser-based system. A proper selection of the relative frequency positions of the two lasers in the proposed OPO frequency chain can significantly reduce the complexity of the OPO network. In Sect. 1, we will describe the basic concept of a two-laser-based OPO frequency chain. A realizable configuration will be examined in Sect. 2. Finally, in Sect. 3, a few applications in precision measurements that can take advantage of the proposed OPO frequency chain will be discussed.

1 Basic concept

The basic structure of a two-laser-based OPO frequency chain is illustrated in Fig. 1. A laser at frequency f_1 is used to pump two OPO frequency dividers with pump-to-out-

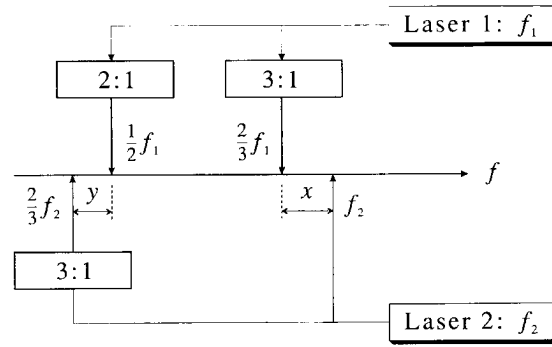


Fig. 1. Basic configuration of a two-laser-based OPO frequency chain

put ratios of 2:1 and 3:1. The 2:1 divider yields the output frequency $(1/2)f_1$, and the 3:1 divider generates the frequency $(2/3)f_1$. (The $(1/3)f_1$ output is also generated but it is not utilized.) It is also possible to replace the 2:1 division with the Second-Harmonic Generation (SHG) of a laser at frequency $(1/2)f_1$, thus generating the pump frequency at f_1 . A second laser whose frequency f_2 is chosen to be close to $(2/3)f_1$ is used to drive a 3:1 OPO divider. The frequency of the generated output $(2/3)f_2$ is therefore close to $(4/9)f_1$.

The relative positions of the four relevant frequencies, $(1/2)f_1$, $(2/3)f_1$, f_2 , and $(2/3)f_2$, are indicated on the frequency axis in Fig. 1, which are related as follows:

$$f_2 = \frac{2}{3}f_1 + x, \quad (1)$$

$$\frac{2}{3}f_2 = \frac{1}{2}f_1 - y. \quad (2)$$

Multiplying (1) by $2/3$ yields

$$\frac{2}{3}f_2 = \frac{4}{9}f_1 + \frac{2}{3}x, \quad (3)$$

which shows that by positioning f_2 close to $(1/3)f_1$, the two 3:1 dividers combine to generate the ratio $(4/9)$ of f_1 . From (2) and (3), we can express the optical frequency f_1 as a function of the difference frequencies x and y ,

$$f_1 = 12x + 18y. \quad (4)$$

The purpose of the three OPO dividers is to create the ratios $(1/2)$ and $(4/9)$ of the calibration frequency f_1 . By measuring the difference frequencies x and y relative to the Cs frequency standard, the absolute value of f_1 is obtained. Once f_1 is measured, f_2 and the four OPO outputs are also calibrated.

Consider $f_1 = 563.8$ THz, which is the second harmonic of YAG at 1064 nm, and, for simplicity, assume $x = y$. From (4), we find that $x = 18.8$ THz. That is, by using two lasers for the OPO network in Fig. 1 and by making two difference-frequency measurements (x and y) of 18.8 THz relative to the Cs clock, the calibration frequency f_1 can be determined accurately. In comparison, a single-laser OPO frequency-counting system that uses a 2:1 and a 3:1 divider generates the ratios $a = 2/3$ and $b = 1/2$, which leads to a difference frequency $(a - b)$

$f = (1/6) f_1 = 94$ THz. This frequency difference is five times larger than that in the proposed two-laser OPO frequency chain. It is clear that an advantage of a two-laser OPO frequency chain is the significant reduction in the frequency difference that needs to be measured. As we shall see in the next section, the benefits of including additional OPOs can be even more significant.

2 Implementation

2.1 Configuration

In principle, any stable laser can be used as the calibration laser f_1 for the proposed OPO frequency chain. In practice, however, the choice of the two pump frequencies depends on the intended application and on the availability of various optical components such as nonlinear crystals. It is best to deploy a simple system consisting of mostly commercially available components. On that basis, we consider using the second harmonic of YAG as the first pump source, with $f_1 = 563.8$ THz. High power (> 0.7 W) cw diode-pumped YAG lasers are commercially available and very narrow linewidths have been obtained by frequency stabilization [8,9]. Second-harmonic conversion efficiency in excess of 80% has been reported at a fundamental wavelength of $1.06 \mu\text{m}$ using MgO:LiNbO₃ [10] and $1.08 \mu\text{m}$ using KTP [11]. Moreover, the YAG and its SHG system can be all-solid-state and compact, which is a desirable feature for a portable frequency chain. It should be noted that the use of a YAG laser and its second harmonic eliminates the need for a 2:1 OPO divider.

The frequency f_2 of the second laser should be near $(2/3)f_1 = 376$ THz, at a wavelength of 798 nm. This is near the peak lasing range of a Titanium-doped Sapphire (Ti:S) laser, which can also be frequency stabilized. A distinct advantage of using a Ti:S laser is its tunability because, as we shall see, an optimum configuration requires that f_2 be varied according to the difference-frequency measurement capability. In the future, the Ti:S laser can be replaced by a diode laser, thus making possible a highly compact and portable frequency chain.

A major challenge in implementing the frequency chain depicted in Fig. 1 is the ability to accurately measure a frequency difference of ≈ 20 THz in the optical domain. Current advances in optical frequency-comb generation have made possible difference-frequency measurement in the THz range and a measurement capability of 10 THz should be feasible in the near future [12,13]. In the proposed system, we intend to solve the problem by subdividing the ≈ 20 THz frequency interval into several smaller intervals that can be accurately measured. By adding an auxiliary set of n tunable 2:1 OPO dividers with outputs centered around $(1/2)f_1$, $n+1$ smaller intervals between $(1/2)f_1$ and $(2/3)f_2$ are created. The number of required auxiliary OPOs depends on the maximum frequency difference that the system is capable of measuring.

Figure 2 shows the schematic of the two-laser-based OPO system. This system is similar to that of Fig. 1 except that the 2:1 divider is now replaced with the YAG laser and its second-harmonic output, and that a set of n auxi-

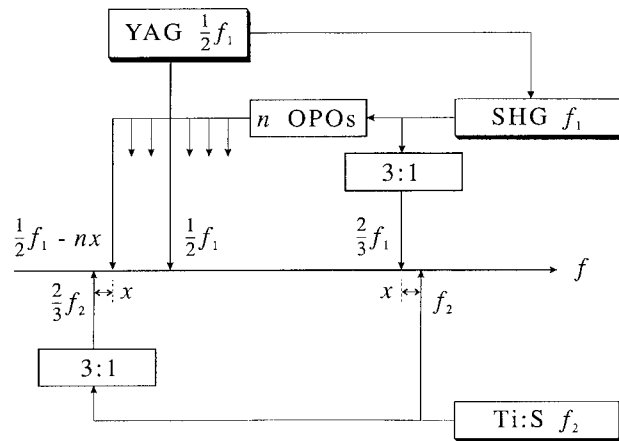


Fig. 2. Schematic of a two-laser-based OPO frequency chain with a set of auxiliary OPOs to facilitate difference-frequency measurements

ary OPOs is used to facilitate the difference-frequency measurement. For simplicity, we assume that all relevant frequency spacings are the same (x), which are to be measured relative to the Cs clock. The two pump frequencies in Fig. 2 are related by

$$f_2 = \frac{2}{3}f_1 + x, \quad (5)$$

$$\frac{2}{3}f_2 + x = \frac{1}{2}f_1 - nx, \quad (6)$$

which yields

$$f_1 = (18n + 30)x, \quad (7)$$

$$f_2 = (12n + 21)x. \quad (8)$$

For $f_1 = 563.8$ THz, Table 1 lists the frequency spacing x , and the frequency and wavelength of the second laser for $n = 0, 3, 4, 5$. The output-frequency range of the n auxiliary OPOs, $(1/2)f_1 \pm nx$, and the corresponding wavelength range are also shown. The case of $n = 0$ is that of the basic configuration of Fig. 1 without an auxiliary set of OPOs and is used here for comparison. It should be pointed out that the operation of the system does not depend on the assumption that the frequency spacings are equal.

Table 1 shows that the frequency spacing x is reduced significantly with the use of a few auxiliary OPOs, dropping from 18.8 THz for $n = 0$ to 5.5 THz for $n = 4$. For a larger n , the decrease in x is much less. For example, one can calculate from (7) that for $n = 10$, $x = 2.7$ THz. In this case, the reduction by a factor of 2 from $x = 5.5$ THz ($n = 4$) to $x = 2.7$ THz ($n = 10$) is obtained at the expense of increased complexity of adding six extra OPOs. If the difference-frequency measurement capability is limited to ≈ 3 THz, then it may be necessary to increase the number of auxiliary OPOs to 10 or more.

We note that f_2 varies only slightly for different n s so that f_2 is always close to $(2/3)f_1$. If an auxiliary OPO needs to be added to or subtracted from the system after it has already been set up, it requires only a minor adjustment to the auxiliary set of OPOs such as a slight change in the

Table 1. Frequency spacing x , frequency f_2 and wavelength λ_2 of second laser, frequency range Δf and the wavelength range $\Delta\lambda$ of the auxiliary set of n OPOs for various values of n . $f_1 = 563.8$ THz

n	x [THz]	f_2 [THz]	λ_2 [nm]	Δf [THz]	$\Delta\lambda$ [nm]
0	18.8	394.5	760	—	—
3	6.7	382.4	784	261.7–301.9	993–1146
4	5.5	381.3	786	259.7–303.9	986–1154
5	4.7	380.4	788	258.3–305.3	982–1161

phase-matching angles of the nonlinear crystals. Because f_2 is nearly constant, the span of the auxiliary set of OPOs, $(1/2)f_1 \pm nx$, varies only slightly for different ns . Therefore, the choice of n depends primarily on how large a frequency difference the system can measure. For the rest of this paper, we will assume $n = 4$, i.e., a measuring capability of at least 5.5 THz.

2.2 Phase-locked OPOs

Wide-span optical frequency combs can be utilized to measure the frequency difference x and to phase lock the OPO system. Resonant Electro-Optic (EO) modulation is a useful technique to generate terahertz optical frequency combs. Efficient modulation at microwave frequencies is obtained by matching the phase velocities of the optical and microwave fields in the modulator substrate and by placing the modulator inside an optical cavity that is resonant for the input beam and the generated side bands. This has been demonstrated to generate hundreds of side bands with a span of several THz, and the optical frequency comb has been used to measure and phase lock optical frequencies separated by a large frequency difference [12, 13].

Figure 3 is a sketch of the phase-locking scheme for the OPO frequency chain by using wide-span EO frequency combs. The example in Fig. 3 consists of an auxiliary set of 3 OPOs and the YAG laser, as represented by four major frequency markers, and two EO frequency combs. Since the higher-frequency outputs of the three OPOs are not needed for phase locking purposes, they are not shown in the sketch. One of the EO frequency combs is generated from the carrier frequency at $(1/2)f_1$ and the other comb from $(1/2)f_1 - 2x$. The OPO output at $(1/2)f_1 - x$ is phase locked to the YAG laser at $(1/2)f_1$ by locking $(1/2)f_1 - x$ to the nearest side band of the YAG-generated EO frequency comb. Therefore, the actual phase locking is between two nearby frequencies separated by at most half of the modulation frequency [13]. To ensure an adequate signal-to-noise ratio for the phase-locked loop, there should be sufficient power in the side band closest to $(1/2)f_1 - x$. Similarly, the EO comb that is generated from the OPO output at $(1/2)f_1 - 2x$ is used to phase lock itself to $(1/2)f_1 - x$ and $(1/2)f_1 - 3x$. In this way, the three OPO outputs are phase locked to the YAG laser by using two EO frequency combs.

For $n = 4$, an additional EO frequency comb generated from the OPO output at $(1/2)f_1 - 4x$ is needed to phase lock itself to $(1/2)f_1 - 3x$ and to $(2/3)f_2$. Therefore, with the use of three wide-span EO frequency combs, the

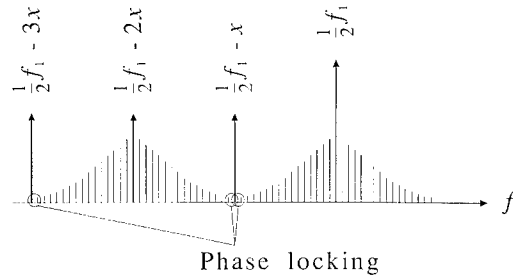


Fig. 3. Diagram showing the use of two EO frequency combs for phase locking a section of the OPO frequency chain. Phase locking takes place between a major frequency marker and its closest side band, as indicated by each of the three circles

YAG laser and the $(2/3)f_2$ OPO output can be phase locked and their frequency difference measured. In addition, a fourth EO frequency comb generated from the Ti:S laser at f_2 is needed to phase lock f_2 and $(2/3)f_1$ so that the entire OPO frequency chain is phase locked. Since the four EO frequency combs are driven by microwave frequencies that are in turn phase locked to the Cs clock, the OPO network is thereby phase locked to the Cs frequency standard, and all the optical frequencies in Fig. 2 are absolutely calibrated. Note that the higher-frequency outputs of the auxiliary set of OPOs are also calibrated because the sum frequency of the higher- and lower-frequency outputs of each OPO must equal the pump frequency f_1 .

2.3 Phase noise

It is useful to estimate the accumulated phase noise of the OPO frequency chain in order to assess how robust the microwave-optical phase-locking system can be. There are four main noise sources: the two lasers, the OPOs, the EO frequency combs, and the optical Phase-Locked Loops (PLLs). In the design of their proposed frequency chain, Nakagawa et al. have shown that the phase-noise contribution of the optical PLLs is small and that the phase noise of the calibration laser dominates [6]. Here, we examine the noise sources of an OPO and of an EO comb generator to show that they too can be small enough to ensure that a cycle slip is unlikely to happen.

The major contributions to the phase noise of an OPO are the phase noise of the pump and the intrinsic phase diffusion noise of the OPO [14]. The pump phase noise is common to all outputs of OPOs that are pumped by the same laser. Consequently, the common-mode pump noise is suppressed to a large degree when the OPO outputs are phase locked. This is the case for the auxiliary set of OPOs which are pumped by the second harmonic of YAG. In the case of the $(2/3)f_1$ and $(2/3)f_2$ OPO outputs, the lower-frequency outputs at $(1/3)f_1$ and $(1/3)f_2$ are not part of the frequency chain and, therefore, the phase noise of the two pump lasers show up in the PLLs that connect one laser to the other. Under appropriate phase-locking conditions, the pump phase noise should become the dominant noise source of the frequency chain [6].

The phase diffusion noise of an OPO is similar to that of a laser, which can be large at low frequencies. It can be

effectively suppressed when it is phase locked to a quiet microwave oscillator. This has been demonstrated in a tunable 2:1 OPO which shows a low-frequency phase noise density of $\approx 0.3 \text{ mrad}/\sqrt{\text{Hz}}$ at a signal-idler beat frequency of 12 GHz [7], limited mostly by the electronic noise in the PLL.

There are two noise sources that affect the optical frequency comb generator. One is the cavity-length fluctuation in the modulator cavity, as pointed out by Nakagawa et al. [6]. Assuming that the cavity length of the high-finesse modulator cavity can be stabilized to within 0.01 nm, the phase noise should be less than 0.02 rad. The second noise source is the phase noise of the microwave signal that drives the EO frequency comb generator.

The phase noise density of the m -th side band of an EO frequency comb due to the microwave oscillator scales quadratically with the side band order m . That is, if $S_\phi(\omega)$ is the phase noise power spectral density of the input modulation field, then the m -th side band will have a power spectral density of

$$S_\phi^m(\omega) = m^2 S_\phi(\omega). \quad (9)$$

For n auxiliary OPOs, the total number of PLLs required for the proposed frequency chain is $n + 2$. Therefore, the total accumulated phase noise variance due to the microwave source(s) is

$$\phi_{\text{total}}^2 = (n + 2)m^2 \bar{S}_\phi B, \quad (10)$$

where \bar{S}_ϕ is the average power spectral density of the modulation field over the PLL bandwidth B .

Consider our example of $n = 4$ and a difference frequency of 5.5 THz. If we assume a modulation frequency of 18 GHz, then it takes $m = 305$ for the EO comb to reach 5.5 THz. In order that a cycle slip does not occur, we can put an upper limit of $\phi_{\text{total}} \leq 1$ rad. For a bandwidth $B = 10$ kHz, this requires an average phase noise density for the microwave source $\bar{S}_\phi \leq -97 \text{ dBc/Hz}$. Typical phase noise density of commercial microwave synthesizers is -80 dBc/Hz , specified at a 10 kHz offset for a microwave frequency of 20 GHz. There are a number of steps that can be taken to keep the total phase noise below 1 rad. Firstly, a microwave source with much lower phase noise can be used. New microwave-cavity designs have produced phase noise densities well below -120 dBc/Hz at an offset of 10 kHz [15]. Secondly, the bandwidth B can be reduced so as to limit the total amount of phase noise. Thirdly, the modulation frequency can be increased so that m is reduced. However, it is likely that at higher microwave frequencies \bar{S}_ϕ increases, thus neutralizing the advantage of reducing m . Lastly, note in (10) that while the phase noise variance is linearly proportional to $n + 2$, it is quadratic with respect to m . It is therefore possible to double the number of PLLs and reduce m by half so that there is a net reduction of a half in the total phase noise variance. Overall, we believe that the most effective reduction in the phase noise is by using an ultralow phase noise microwave source.

2.4 Nonlinear crystals

The viability of the proposed OPO frequency chain depends on the availability of nonlinear crystals that can

efficiently generate the required OPO outputs. These include the auxiliary set of tunable 2:1 OPOs and the two 3:1 OPOs. It is well known that potassium titanyl phosphate (KTP) can be non-critically type-II phase matched for 1064 nm SHG [16]. Therefore KTP is phase matchable at the same angle for a frequency-degenerate 2:1 OPO pumped at 532 nm. Indeed, the outputs of the entire auxiliary set of tunable 2:1 OPOs in Fig. 2 can be generated by non-critically type-II phase-matched KTP crystals. Type-II phase matching is important in this case because it eliminates the cluster-mode hopping that is common in nearly degenerate type-I phase-matched OPOs [17, 18]. Also, KTP has a wide temperature tolerance and a large acceptance angle that are desirable for stable operation of an OPO frequency divider.

Cesium Titanyl Arsenate (CTA) is a nonlinear crystal that can be non-critically type-II phase matched for 3:1 frequency division pumped at 532 nm [19]. CTA is an arsenate isomorph of KTP and therefore is similar to KTP in many ways: a nonlinear coefficient of the same magnitude, a wide temperature bandwidth, and a large acceptance angle. It is expected that a cw OPO based on CTA should have a threshold and tuning behavior similar to a KTP OPO. A recent three-wave mixing experiment [20] confirms that CTA has approximately the same magnitude in its nonlinear coefficients as KTP and it can be phase matched at an angle of $\theta = 90^\circ$, $\phi \approx 48^\circ$ for 3:1 division pumped at 532 nm. The experiment also shows that further improvement in the crystal quality is needed before cw parametric oscillation can be achieved.

Rubidium Titanyl Phosphate (RTP) is another isomorph of KTP that can be non-critically phase matched at $\phi \approx 31^\circ$ to permit 3:1 frequency division pumped at $f_2(\lambda_2 \approx 787 \text{ nm})$ [21]. As in the case of CTA, the nonlinear coefficients, temperature bandwidth, and acceptance angle of RTP are similar to those of KTP. Both CTA and RTP are relatively new crystals and their crystal quality are not as good as that of KTP.

In 3:1 frequency division, the exact ratio of 3:1 is obtained by phase locking the $(2/3)f$ output and the second harmonic of the $(1/3)f$ output. The second harmonic of $(1/3)f$ can be generated either external or internal to the OPO cavity with a doubling crystal. For the 532 nm pumped 3:1 divider, the 1596 nm radiation can be doubled with a CTA crystal at a phase matching angle of $\theta \approx 82^\circ$ and $\phi = 0^\circ$. Since θ is close to the non-critical phase-matching angle of 90° , the walkoff is moderate with a calculated walkoff angle of $\approx 0.46^\circ$. Similarly, the second harmonic of $(1/3)f_2$ at $\approx 2359 \text{ nm}$ can be generated using a CTA crystal cut at $\theta \approx 87^\circ$ and $\phi = 0^\circ$, with an estimated walkoff angle of 0.16° . It is clear that high-quality CTA crystals are essential to the realization of the two 3:1 frequency dividers in the proposed OPO-based optical frequency chain.

2.5 Pump powers

Another practical aspect of the proposed frequency chain is the amount of optical pump powers that are required to drive the two 3:1 OPOs and the auxiliary set of four OPOs. Assuming that the CTA and RTP crystals will be

of good quality approaching that of KTP, the minimum threshold should be in the range of 25–40 mW. For pumping the OPOs at 1.5 times above threshold, ≈ 0.3 W of power at 532 nm should be adequate. This should be obtainable from SHG of YAG at a fundamental power level of 0.5 W or higher [11]. In a worst-case scenario in which the required operating pump power is higher or the SHG conversion efficiency is lower, two phase-locked YAG lasers would provide the required pump power. The modest power that is required at 787 nm can be easily obtained from a low-power Ti:S laser or diode laser.

3 Applications

The establishment of an optical-microwave frequency chain permits the absolute optical frequencies of f_1 and f_2 , as well as all the frequencies derived from the two frequencies, to be accurately known relative to the Cs primary frequency standard. As a result, the OPO outputs and the side bands of the EO frequency combs serve as calibrated optical frequency markers for measuring other optical frequencies. For the proposed system in Fig. 2, the calibrated spectral regions are: 532 nm [f_1], 786–798 nm [$f_2 \rightarrow (2/3)f_1$], 986–1179 nm [$(1/2)f_1 + 4x \rightarrow (2/3)f_2$], 1596 nm [$(1/3)f_1$], and 2359 nm [$(1/3)f_2$]. By use of nonlinear sum- and difference-frequency mixing, it should be possible to measure a number of optical frequencies of metrological or spectroscopic importance with unprecedented accuracy. Some of the measurements that can benefit from the OPO frequency chain are briefly discussed below.

3.1 CH_4 -stabilized HeNe at 3.39 μm

The methane-stabilized HeNe laser at 3.39 μm (88.376 THz) is one of the most accurately known optical frequencies and it has been measured directly relative to the Cs clock using a traditional frequency chain [1, 2]. It is therefore interesting to measure the 3.39 μm line using the OPO frequency chain and compare it with the value obtained by the traditional frequency chain. By mixing the 1064 nm radiation of YAG with the 3.39 μm laser it yields a difference frequency of 193.5 THz at the wavelength of 1550 nm. The difference-frequency output can then be compared with the $(1/3)f_1$ output of the 532 nm driven OPO which has a frequency of 187.9 THz (1596 nm). The frequency difference between the two wavelengths, 1550 and 1596 nm, is 5.6 THz, which is measurable with the use of an EO frequency comb. Difference-frequency mixing of 1.06 and 3.39 μm laser lines can be accomplished in another isomorph of KTP: Potassium Titanyl Arsenate (KTA) at $\theta = 90^\circ$, $\phi \approx 61^\circ$ [21].

3.2 1S–2S transition of hydrogen

One of the most fundamental measurements in atomic spectroscopy is the hydrogen's 1S–2S two-photon transition at 2468 THz. Its absolute frequency accuracy is

important for checking the precision of quantum electrodynamics calculations and for obtaining new accurate values of a number of fundamental constants [22]. The pump radiation for the two-photon transition is usually generated by doubling the frequency at 617 THz (486 nm) which, in turn, can be obtained by doubling a Ti:S laser at 308 THz (972.6 nm). This Ti:S laser frequency is located only 4 THz from the $(1/2)f_1 + 4x$ output (304 THz, 987 nm) of the auxiliary set of OPOs. Therefore, a straightforward frequency comparison between the two frequencies using an EO frequency comb should permit the absolute frequency measurement of the 1S–2S transition frequency.

3.3 Two-photon transition of rubidium

Another interesting two-photon transition is that of rubidium (Rb) between the $5S_{1/2}$ and $5D_{3/2}$ levels, which has recently been measured absolutely with an uncertainty of 1.3×10^{-11} [23]. It is a potential optical frequency standard in the near-IR region. The drive frequency for this two-photon Rb transition at 385.5 THz (778 nm) is separated from the Ti:S pump laser f_2 (787 nm) of the OPO frequency chain by 4 THz. Again, an EO frequency comb will enable the frequency difference between f_2 and the two-photon pump frequency to be measured.

3.4 I_2 -stabilized HeNe at 633 nm

The iodine-stabilized HeNe laser at 633 nm is a secondary optical frequency standard located in the red spectral region and provides a convenient wavelength marker in the visible region. The sum frequency mixing of $(1/2)f_1$ at 1064 nm and $(1/3)f_1$ at 1596 nm yields $(5/6)f_1$ at 638 nm which is 4 THz away from the 633 nm line. Since the 638 nm output is derived entirely from the YAG laser, one should note that even without an optical-microwave frequency chain, the frequency comparison here provides a measurement of the YAG laser frequency (whose second harmonic can be stabilized to another iodine line [8]) relative to the red HeNe laser. A CTA crystal set at $\theta = 90^\circ$, $\phi \approx 23^\circ$ can be used to perform the required sum-frequency mixing.

3.5 Calcium transition at 657 nm

Another interesting spectroscopic line in the red spectral region is the intercombination transition between the ground state 1S_0 and the 3P_1 state of calcium at 657 nm [24]. The narrow linewidth of the line makes it a prime candidate for an optical frequency standard. The sum frequency mixing of $(2/3)f_1$ at 1596 nm and $(1/2)f_1 - 2x$ at 1108 nm yields an output at 654 nm, which is 2 THz from the 657 nm line. As in the case of the HeNe line at 633 nm, a CTA crystal can be used to generate the 654 nm radiation by using a phase-matching angle of $\theta = 90^\circ$, $\phi \approx 6^\circ$.

4 Conclusion

We have proposed a two-laser-based parallel network of OPOs for use as an optical-to-microwave frequency chain to provide an absolute optical frequency-measurement capability over a broad spectrum. The parallel network confines the operating wavelengths of the chain to the near-IR spectral region. With the use of two pump lasers instead of one laser, the number of required OPO stages is reduced. The proposed OPO frequency chain can be constructed using mostly readily available components in the 800–1600 nm spectral region. The size of the network is dependent on the difference-frequency measurement capability. The higher the difference frequency that one can measure, the smaller the number of OPOs that are required. Hence, the development of wide-band optical frequency-comb generation is critical to the implementation of the proposed frequency chain. At the same time, it is also important to have high-quality nonlinear optical crystals that can be used to generate the various OPO outputs, especially the CTA and RTP crystals for 3:1 dividers. Research in the area of quasi-phase-matched nonlinear materials is particularly relevant because they can be fabricated to phase match at any user-specified wavelength [25–27]. Moreover, the use of quasi-phase matching in waveguides may eventually reduce the OPO system to a very compact, and perhaps even a single-chip, device.

The proposed frequency chain is potentially useful for many applications in metrology and spectroscopy because there is a broad spectral range in which the frequency is either calibrated or can be calibrated using an additional frequency-mixing stage. New development in the Cs-clock technology such as an atomic Cs fountain may usher in a new era of ultrahigh resolution of the order of 10^{-16} [3]. In this case, the proposed OPO frequency chain can be utilized to transfer this ultrahigh accuracy in the rf regime to the optical regime. Conversely, the fractional accuracy of future optical frequency standards with very high line Q s can be transferred to the rf regions by using the same OPO frequency chain.

Acknowledgement. This research was supported by the U.S. Army Research Office under grant DAAH04-93-G-0399.

References

1. D.A. Jennings, C.R. Pollock, F.R. Petersen, R.E. Drullinger, K.M. Evenson, J.S. Wells, J.L. Hall, H.P. Layer: *Opt. Lett.* **8**, 136 (1983)
2. C.O. Weiss, G. Kramer, B. Lipphardt, E. Garcia: *IEEE J. QE-* **24**, 1970 (1988)
3. K. Gibble, S. Chu: *Metrologia* **29**, 201 (1992)
4. N.C. Wong: *Opt. Lett.* **17**, 1155 (1992)
5. H.R. Telle, D. Meschede, T.W. Hänsch: *Opt. Lett.* **15**, 532 (1990)
6. K. Nakagawa, M. Kourogi, M. Ohtsu: *Appl. Phys. B* **57**, 425 (1993)
7. D. Lee, N.C. Wong: *Opt. Lett.* **17**, 13 (1992)
8. A. Arie, S. Schiller, E.K. Gustafson, R.L. Byer: *Opt. Lett.* **17**, 1204 (1992)
9. N.M. Sampas, E.K. Gustafson, R.L. Byer: *Opt. Lett.* **18**, 947 (1993)
10. R. Paschotta, P. Kürz, R. Henking, S. Schiller, J. Mlynek: *Opt. Lett.* **19**, 1325 (1994)
11. Z.Y. Ou, S.F. Pereira, E.S. Polzik, H.J. Kimble: *Opt. Lett.* **17**, 640 (1992)
12. M. Kourogi, K. Nakagawa, M. Ohtsu: *IEEE J. QE-* **29**, 2693 (1993)
13. L.R. Brothers, D. Lee, N.C. Wong: *Opt. Lett.* **19**, 245 (1994)
14. R. Graham, H. Haken: *Z. Phys.* **210**, 276 (1968)
15. G. J. Dick: In *Proc. IEEE Frequency Control Symp.*, IEEE Cat. No.92CH3083-3, (IEEE, New York 1992) pp. 349–355
16. J.D. Bierlein, H. Vanherzeele: *J. Opt. Soc. Am. B* **6**, 622 (1989)
17. D. Lee, N.C. Wong: *J. Opt. Soc. Am. B* **10**, 1659 (1993)
18. R.C. Eckardt, C.D. Nabors, W.J. Kozlovsky, R.L. Byer: *J. Opt. Soc. Am. B* **8**, 646 (1991)
19. L.T. Cheng, L.K. Cheng, J.D. Bierlein, F.C. Zumsteg: *Appl. Phys. Lett.* **63**, 2618 (1993)
20. B. Lai: A tunable light source at 1.6 nm by difference – frequency mixing in cesium titanyl arsenate. M.S. Thesis, Massachusetts Institute of Technology, Cambridge, MA (1995) (unpublished)
21. L.T. Cheng, L.K. Cheng, J.D. Bierlein: *SPIE Proc.* **1863**, 43 (1993)
22. T. Andrae, W. König, R. Wynands, D. Leibfried, F. Schmidt-Kaler, C. Zimmermann, D. Meschede, T.W. Hänsch: *Phys. Rev. Lett.* **69**, 1923 (1992)
23. F. Nez, F. Biraben, R. Felder, R. Millerioux: *Opt. Commun.* **102**, 432 (1993)
24. N. Ito, J. Ishikawa, A. Morinaga: *J. Opt. Soc. Am. B* **7**, 1388 (1991)
25. M.M. Fejer, G.A. Magel, D.H. Jundt, R.L. Byer: *IEEE J. QE-* **28**, 2631 (1992)
26. M. Yamada, N. Nada, M. Saitoh, K. Watanabe: *Appl. Phys. Lett.* **62**, 435 (1993)
27. L.E. Myers, G.D. Miller, R.C. Eckardt, M.M. Fejer, R.L. Byer: *Opt. Lett.* **20**, 52 (1995)

Accession For	
NTIS GRA&I	<input checked="" type="checkbox"/>
DTIC TAB	<input type="checkbox"/>
Unannounced	<input type="checkbox"/>
Justification	
By	
Distribution/	
Availability Codes	
Dist	Avail and/or Special
A-1	20